Research Article **Rev. Cong. Sci. Technol., Vol. 5, No. 2, pp. 797-808 (2026)**

OPEN ACCESS

Revue Congolaise des Sciences & Technologies

ISSN: 2959-202X (Online); 2960-2629 (Print)

https://www.csnrdc.net/

Kinetic and thermodynamic studies adsorption of Methylene Blue (MB) in aqueous solution on a biosorbent based on *Persea americana* Mill Kernels

[Études cinétiques et thermodynamiques de l'adsorption du bleu de méthylène (MB) en solution aqueuse sur un bioadsorbant à base de noyaux de *Persea americana* Mill]

Emmanuel Oria Mateso, Anatole Kia Mayeko Kifuani*, Bernick Wembolowa Tshene, Kifline Milebudi Kifuani, Léon Longo Khonde, Pitchou Bokolombe Ngoy & Gracien Bakambo Ekoko

Laboratory of Physical Organic Chemistry, Water and Environment, Department of Chemistry and Industry, Faculty of Sciences and Technology, University of Kinshasa, P.O. Box 190 Kinshasa XI, Democratic Republic of the Congo

Abstract

This study investigated the removal of methylene blue (MB) from aqueous solution via adsorption onto a biosorbent derived from *Persea americana* Mill (PAB) kernels. Adsorption was studied in batch mode by varying contact time (0 to 390 min), initial concentration of MB (1 mg/L to 100 mg/L), and the temperature (301 K to 323 K). The results showed that the adsorption capacity and percentage of adsorption at different temperatures increase with contact time. This increase is due to the availability of free adsorption sites on the surface of the biosorbent. The kinetic and equilibrium results obtained in this study show that the pseudo-second-order model (R^2 = 0.8422) is a better fit than the pseudo-first-order model (R^2 = 0.8149) for describing the adsorption kinetics of MB on the PAB biosorbent. The Langmuir equilibrium model (R^2 = 0.7771) better describes the adsorption equilibrium of MB on the PAB biosorbent compared to the Freundlich model (R^2 = 0.7752). The Langmuir separation parameter R_L and the Freundlich 1/*n* parameter less than 1 suggest that the adsorption of MB on the PAB biosorbent is favorable. The determined ΔG values for each temperature show that the adsorption of MB onto PAB is favorable and spontaneous. The positive ΔH° values indicate that the adsorption is endothermic and physical.

Keywords: *Persea americana*, Methylene Blue, Adsorption, Biosorbent, Isotherm, Kinetic

Résumé

L'élimination du bleu de méthylène (BM) en solution aqueuse par adsorption sur un bioadsorbant à base des noyaux de *Persea americana* Mill (PAB) a fait l'objet de cette étude. L'adsorption a été étudiée en mode batch en variant le temps de contact (0 min à 390 min), la concentration initiale de la solution de BM (1 mg/L à 100 mg/L) et la température (301 K à 323 K). Les résultats obtenus ont montré que la capacité d'adsorption et le pourcentage d'adsorption à différentes températures augmentent avec le temps de contact. Cette augmentation est due à la disponibilité des sites libres d'adsorption à la surface du bioadsorbant. Les résultats de la cinétique et d'équilibre obtenus montrent que le modèle pseudo-second ordre (R^2 = 0,8422) est meilleur comparé au modèle pseudo-premier ordre (R^2 = 0,8149) pour décrire la cinétique d'adsorption du MB sur le biosorbant PAB. Le modèle d'équilibre de Langmuir (R^2 = 0,7771) décrit mieux l'équilibre d'adsorption du MB sur le bioadsorbant PAB par rapport au modèle de Freundlich (R^2 = 0,7752). Le paramètre de séparation de Langmuir R_L et le paramètre 1/*n* de Freundlich, inférieur à 1, suggèrent que l'adsorption de MB sur le bioadsorbant PAB est favorable. Les valeurs de $\Delta G < 0$, pour chaque température, montrent que l'adsorption de BM sur PAB est spontanée et favorable. Les valeurs positives de $\Delta H° < 40$ kJ mol^{-1} obtenues indiquent que l'adsorption est endothermique et essentiellement physique.

Mots clés: *Persea americana*, Bleu de méthylène, Adsorption, Biosorbant, Isotherm, Kinetic

*Auteur correspondant : Anatole Kia Mayeko Kifuani, (anatolekifuani@gmail.com). Tél. : (+243) 998 229 987

https://orcid.org/0009-0002-2349-5846; Reçu le 08/04/2026 ; Révisé le 05/05/2026 ; Accepté le 27/05/2026

DOI : https://doi.org/10.59228/rcst.026.v5.i2.286

1. Introduction

Various human activities are major sources of water pollution. Among the main water pollutants are organic dyes, pesticides, organic solvents, and trace metal elements. Several industries use organic dyes to color textiles, leather, paper, plastics, cosmetics, food, and pharmaceutics, as well as for printing inks and applications in photography or scientific research. These compounds are also used in biology, medicine, and in other works (Kifuani et al., 2025; Razia et al., 2022). Organic dyes can have significant effects on both human health and the environment. Regarding human health, some synthetic dyes, particularly azo dyes, can break down aromatic amines such as benzidine, which are known carcinogens associated with an increased risk of bladder, liver, and spleen cancers. Direct contact or inhalation of these compounds can also cause allergic reactions, skin dermatitis, eczema, asthma, and irritation of the eyes and respiratory tract. In the environment, the discharge of colored effluents causes serious problems even at low concentrations (Merbouh et al., 2020; Amal et al., 2024; Ibrahim et al., 2026). Dye strongly colors water, reducing light penetration and inhibiting photosynthesis in aquatic plants and algae. Many dyes are directly toxic to aquatic life, affecting fish, crustaceans, and microorganisms. Furthermore, certain dyes and their degradation products can bioaccumulate in food chains, leading to long-term ecological risks. Methylene blue is a widely used organic dye with several important applications in medicine, pharmacy, biology, aquaculture, and industries. In the environment, methylene blue is toxic to fish and invertebrates at concentrations from 10 to 50 mg/L and inhibits algal growth. It has low biodegradability, persists in water bodies, and resists removal by conventional wastewater treatment.

The removal of methylene blue, as well as other organic dyes, is therefore necessary. Several methods and techniques are used for the removal of methylene blue or other organic dyes from wastewater. The methods for removing organic dyes from water can be biological, chemical, or physical. These methods include the following techniques: adsorption, advanced oxidation, chemical and electrochemical oxidation, coagulation, flocculation, Fenton electron process, microbial and fungal decolorization, photocatalysis, nanofiltration, ozonation, and reverse osmosis (Narayana et al., 2019; Elie et al., 2024; Alhawtali et al., 2024). Of all these techniques, adsorption has proven to be a very effective technique. Activated carbon is the most widely used adsorbent for water treatment. But for the treatment of wastewater, its high production cost and its difficult regeneration make its use expensive.

Currently, several studies report the use of biomass from agricultural waste for trials to remove organic dyes from water. This biomass includes apricot stones, banana pith, coconut coir dust, cotton stalk, hazelnut shell, green pea peels, mango seed kernel, oil palm shell, orange peel, *Curcumeropsis manni* shells, and *Manihot esculenta* kernels (Kifuani et al., 2018b; Tshene et al., 2024). These materials contain organic substances such as polyphenols, lignin, tannins, flavonoids, cellulose, starch, and proteins, which provide active surface functions, such as carboxylic acid, ketone, aldehyde, phenol, lactone, and pyrone, responsible for the adsorption of organic dyes or other pollutants on their surface. In a recent article (Mateso et al., 2025), the adsorption of methylene blue onto a biosorbent derived from *Persea americana* kernels was studied under various conditions, including biosorbent mass, contact time, concentration, and pH of the methylene blue solutions. This study investigated the effects of contact time, initial concentration, and temperature for the same biosorbent to determine the influence of temperature on adsorption.

2. Material and methods

2.1. Biosorbent preparation

The study was carried out using *Persea americana* seeds from Mbanza Ngungu, in the Kongo Central Province, Democratic Republic of the Congo. The biomass of seeds was first sun-dried, then oven-dried at 105°C (DESPATCH Oven Co., type Elect) to eliminate the water content. The obtained dry matter is ground in a grinder (industrial high-speed grinder 100 A) and then sieved to obtain a powder with a particle size ≤ 500 µm. The *Persea americana* biosorbent (PAB) thus obtained was stored in airtight packaging and placed in a desiccator at laboratory temperature (28°C) to keep it free from moisture contact and oxidation (Kifuani et al., 2018b).

2.1.1. Characterization of the biosorbent

Various physicochemical parameters of the biosorbent (PAB) were determined and included grain size, moisture content, dry matter, ash content, surface

chemical functional groups, pH at zero point of charge, specific surface area, and the maximum observed capacity.

2.1.2. Grain size

The grain size of the grains was determined by sifting using a sieve (Retsch AS200 Tap).

2.1.3. Moisture content and dry matter

The moisture content (*M*) and the dry matter (*DM*) of the biosorbent were determined using the gravimetric volatilization method. For this purpose, 5 g of the biosorbent were heated (105°C) in an oven for 48 hours; after that, the residue was weighed. The moisture content (%*M*) of the biosorbent is then given by equation 1 (Ajala et al., 2024).

$$\%M = \frac{(m_1 - m_2) \cdot 100}{m_1} \quad [1]$$

Where m_1 and m_2 are the weights of the biosorbent before and after steaming, respectively.

The dry matter level (%*DM*) is calculated after deducting the moisture content (%*M*) from 100% of the initial sample.

2.1.4. Ash content

Ash content of the biosorbent was determined by calcining 5 g of sample in a muffle furnace at 550°C (Naber, model N7H) for 8 hours to obtain the ash. The ash content (%*A*) was calculated using the following equation 2 (Basma et al., 2024).

$$\%A = \frac{(m_4 - m_0) \cdot 100}{(m_3 - m_0)} \quad [2]$$

Where, m_4 the weight of the ash and empty crucible after calcination; m_3, the weight of the sample and empty crucible before calcination; and m_0, the weight of the empty crucible.

2.1.5. Surface chemical functional group determination

Surface functional groups were determined using the Boehm method, which corresponds to acid-base titration. Acidic and basic groups were quantified in their entirety. To do this, 1 g of biosorbent was contacted with 50 mL of a 0.1 N solution of the base (NaOH) and 0.1 N of the salts ($NaHCO_3$ and Na_2CO_3) for 72 hours with stirring to determine acidic or phenolic groups, then with 50 mL of a 0.1 N HCl solution to determine basic groups. Subsequently, the different solutions were filtered. Then, 10 mL of the filtrate from each solution was titrated. The basic solution was titrated with 0.1 N HCl, and the acidic solution with 0.1 N NaOH. The desired function is given, in milliequivalents per gram, by the following equation 3 (Kouadio et al., 2022):

$$nmeq = N_iV_i - N_fV_f \quad [3]$$

Where, nmeq the number of milliequivalent grams that have reacted, N_iV_i number of milliequivalent grams before the reaction, and N_fV_f the number of milliequivalent grams after the reaction.

2.1.6. Determination of pHZPC

The pH at the point of zero charge (pH_{ZPC}) was determined using the Boehm method, also known as the pH drift method. For this purpose, 100 mL of 0.01 mol/L NaCl solutions are placed in different adsorbers (LACOPE ADX), and the pH of these solutions is adjusted from 2 to 12 by the addition of 0.1 N HCl or 0.1 N NaOH solutions to adjust the acidic or basic solutions, respectively. 1000 mg of biosorbent was then added to each solution, and the suspension was stirred for 72 h and centrifuged at 3000 rpm (Centrifuge Labofuge 200 Heraeus). The final pH of each solution was determined using a pH-meter (Hanna Instruments). The point of intersection of the curve obtained by plotting the final pH as a function of the initial pH of each solution determines the pH_{ZPC} (Musah et al., 2020).

2.1.7. Determination of the maximum observed capacity (Q_{mo}) and specific surface area (S_{MB}).

The specific surface area of the biosorbent was determined by adsorption of methylene blue using the Kifuani volume variation method (KVVM). This method consists of studying the adsorption of methylene blue at equilibrium time, using a low mass of adsorbent. For this purpose, to 5 mg of adsorbent, increasing volumes (100 mL to 1000 mL) of the MB solution 50 mg/L are added. The suspension is stirred at the equilibrium time previously determined experimentally.

The determination of the residual concentration of the supernatant by UV-spectrophotometry makes it possible to calculate the maximum adsorption capacity (Q_m) and the maximum adsorption capacity (%m*Ads*) using equations 4 to 6. The curve obtained by plotting the maximum adsorption capacity (Q_m) as a function of the volume (V) of the MB solution makes it possible to determine the true maximum adsorption capacity, which we call the maximum observed adsorption capacity (Q_{mo}), the others being apparent maximum capacities (Q_m). The maximum observed adsorption capacity is given by the plateau of this curve (Kifuani, 2013; Kifuani et al., 2018a).

$$Qm = \frac{(C_o - C_e)\,V}{m_B} \quad [4]$$

$$\%\, mAds = \frac{C_o - C_e}{C_o} \times 100 \quad [5]$$

With, Q_m being the maximum adsorption capacity of the biosorbent (mg g^{-1}), C_o the initial concentration of methylene blue solution (mg L^{-1}), C_e the residual or equilibrium concentration (mg L^{-1}), V the volume of the methylene blue solution (L), and %mo*Ads* the maximum observed adsorption percentage.

The specific surface area (S_{MB}) is then calculated according to the following equation 6 (Kifuani , 2013):

$$S_{MB} = Q_{mo}.\ N_A.\ S \quad [6]$$

Where, S_{MB} is the specific surface area determined using MB as adsorbate ($m^2\ g^{-1}$), Q_{mo} the maximum observed adsorption capacity (mg g^{-1}), N_A the Avogadro number ($6.022 \times 10^{23}\ mol^{-1}$), and S the area occupied by a MB molecule (175 Å²).

2.2. Adsorbate and adsorbate solutions

In this study, methylene blue dye was used as a model of organic dye because of its flat surface known in the literature (175 Å²). His IUPAC name is 3,7-Bis(dimethylamino)phenothiazine-5-ium chloride. Methylene blue is a cationic dye having the chemical formula $C_{16}H_{18}N_3SCl$ and *Mw* of 319.852 g mol^{-1}. All reagents used in this study were from Merck and were used without further purification. Figure 1 gives the structure of methylene blue dye.

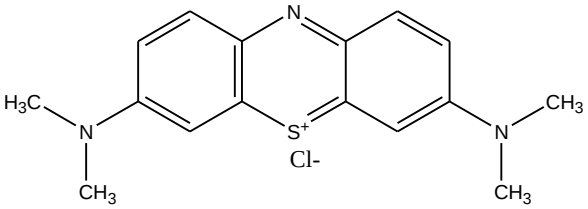

Figure 1. Chemical structure of methylene blue

The preparation of MB solutions was made by dissolving MB crystals in distilled water and diluting the resulting solution to obtain solutions ranging from 1 mg L^{-1} to 100 mg L^{-1}. The MB solutions, before and after adsorption, were analyzed using a UV-Vis spectrophotometer (HACK Spectrophotometer, SP, model 1105) at their self-maximum wavelength determined experimentally at their natural pH (pH = 6.05). The residual concentration of MB solution was calculated using the Beer-Lambert equation (equation 7) (Kifuani et al., 2018a; Raiyyaan et al., 2021).

$$A = \varepsilon.l.C \quad [7]$$

With, A the absorbance, ε the molar absorption coefficient (L mg^{-1} cm^{-1}), l the thickness of the cell (1 cm), and C the concentration of the MB (mg L^{-1}).

2.3. Batch adsorption experiments

The adsorption tests were carried out in batch experiments with adsorbers (LACOPE ADS) using 100 mL of MB solutions and a biosorbent mass of 600 mg, the optimal mass determined in previous research (Mateso et al., 2025). The concentrations of MB solutions were varied from 5 mg/L to 100 mg, and the temperature was varied from 301 K to 323 K. All adsorption tests were performed at the self-equilibrium pH (6.05) of the solutions. Several bioadsorbent samples were weighed using an analytical balance (HEB-E 303). After stirring for the required time, the suspension was centrifuged at 3000 rpm for 30 minutes, and the supernatant was analyzed with a UV-Vis spectrophotometer at the appropriate wavelength (662 nm) to determine the residual concentration of the MB solution. Each experiment is repeated three times to determine the absolute error. The adsorption capacity (Q_e) and the adsorption percentage (%*Ads*) were calculated using equations 8 and 9, respectively (Mobalaji *et al*., 2021):

$$Q_e = \frac{(C_o - C_e)\,V}{m_B} \quad [8]$$

$$\%\ Ads = \frac{C_o - C_e}{C_o} \times 100 \quad [9]$$

With, Q_e being the apparent adsorption capacity or the equilibrium capacity of the biosorbent (mg g^{-1}), C_o the initial concentration of MB solution (mg L^{-1}), C_e the residual or equilibrium concentration (mg L^{-1}), V the volume of MB solution (L), and %Ads the adsorption percentage.

2.4. Adsorption kinetics

The modeling of the adsorption kinetics was done according to the Lagergren kinetic model (Mekky et al., 2020) using the kinetic equations of the surface reaction of pseudo-first-order and pseudo-second-order developed by Kifuani (2013) (Equations 10 and 11):

Kifuani pseudo-first-order kinetic model:

$$\ell n \frac{q_e}{(q_e - q_t)} = k_1 t \quad [10]$$

With, q_e being the adsorption capacity at equilibrium (mg g^{-1}), q_t the adsorption capacity at time t (mg g^{-1}), q_e-q_t the adsorption capacity of free sites, t the time (s), and k_1 the constant rate of pseudo-first-order reaction (min^{-1}). The plot of $\ell n \frac{q_e}{(q_e - q_t)}$ versus t gives a line whose slope corresponds to k_1, the rate constant of a pseudo-first-order reaction.

Kifuani pseudo-second-order kinetic model:

$$\frac{q_t}{q_e(q_e - q_t)} = k_2 t \quad [11]$$

With, k_2 being the rate constant of the pseudo-second-order reaction (g mg^{-1} min^{-1}). The plot of

$\frac{q_t}{q_e(q_e - q_t)}$ versus t gives a line whose slope corresponds to k_2, the rate constant of the pseudo-second-order reaction.

2.5. *Adsorption isotherms*

The modeling of the adsorption equilibrium was done using the Langmuir and Freundlich models given by the following equations 12 to 14 (Alouani et al., 2018; Mekhalef et al., 2018):

Langmuir model:

$$\frac{1}{Q_e} = \frac{1}{Q_m} + \frac{1}{Q_m K_L} \cdot \frac{1}{C_e} \quad [12]$$

Where, Qe being the apparent adsorption capacity of the biosorbent (mg g^{-1}), Q_m the adsorption capacity at saturation or maximum adsorption capacity (mg g^{-1}), K_L the equilibrium constant adsorption (L mg^{-1}), and Ce the equilibrium concentration. The plot of $1/Q_e$ versus $1/C_e$ gives a line that allows determining Q_m and K_L from the intercept and slope, respectively.

The Langmuir separation parameter (R_L) was calculated using equation 13 (Hajir et al., 2024):

$$R_L = \frac{1}{1 + K_L C_o} \quad [13]$$

With, K_L being the Langmuir constant (L mg^{-1}) and C_o the initial dye concentration (mg L^{-1}).

Freundlich model:

$$\log Q_e = \log K_F + \frac{1}{n} \log C_e \quad [14]$$

With Q_e being the adsorption capacity at equilibrium (mg g^{-1}), K_F the adsorption constant (Freundlich constant), C_e the concentration of the adsorbate at equilibrium (mg L^{-1}), and n the Freundlich constant characterizing the affinity of the solute for the adsorbent (affinity parameter). The plot of log Q_e versus log C_e gives a line that allows to determine K_F and $1/n$ from the intercept and slope, respectively.

2.6. *Thermodynamic parameters*

Plotting $\ln K_d = f(1/T)$ yields a straight line whose slope allows the calculation of the standard enthalpy ($\Delta H°$), and the standard entropy ($\Delta S°$) is obtained from the y-axis. These two parameters allow the calculation of the standard Gibbs free energy of adsorption (ΔG°) and the Gibbs free energy (ΔG) at different temperatures, using the Van T'hoff equation 14 (Amal et al., 2024):

$$\Delta G° = - RT \ln K_d \quad [14]$$

Where, R is the gas constant (J mol^{-1} K^{-1}), T the absolute temperature (K), and K_d the distribution coefficient (mg L^{-1}).

$$ln K_d = \frac{\Delta S°}{R} - \frac{\Delta H°}{RT} \quad [15]$$

3. RESULTS

3.1. *Characteristics of the biosorbent PAB*

The physicochemical properties summarized in Table I show that PAB has a specific surface area of 102.86 m^2/g and a maximum observed adsorption capacity of 31.22 mg/g. The pH of zero potential charge (pH_{ZPC}) of the adsorbent is 4.27. The surface functional groups determined by the Boehm method indicate the presence of carboxylic, lactonic, and phenolic acid groups and basic groups (table II).

Table I. Physicochemical characteristics of the PAB biosorbent

Parameters	Values
Particle size (mm)	≤ 1.00
Ash content (%)	3.28
Moisture content (%)	6.50
Dry matter (%)	93.50
pH_{zpc}	4.27
Q_{mo} (mg g^{-1})	31.22
Specific area, S_{MB} (m^2 g^{-1})	102.86

Table II. Surface chemical functional groups of PAB

Functions		Number of milliequivalent-grams
Acid:	Carboxylic acid	0.77 meq/g
	Lactone	0.57 meq/g
	Phenol	0.27 meq/g
	Total:	**1.61 meq/g**
Basic		0.22 meq/g

3.2. *Temperature effect*

The effect of temperature on the adsorption of PAB by MB was studied by varying the temperature from 301 K to 323 K. The results obtained, shown by figures 2 and 3, show an increase in the adsorption capacity and percentage adsorption with rising temperature. In fact, increasing the temperature from

301 K to 323 K slightly increased the adsorption capacity from 8.097 mg/g to 8.222 mg/g, as shown in table III.

Table III. Values of Q_m and $\%_m Ads$ at different temperatures

T (K)	Q_m(mg/g)	$\%_m Ads$
301	8.10	97.17
308	8.14	97.17
313	8.15	97.67
318	8.21	98.50
323	8.22	98.67

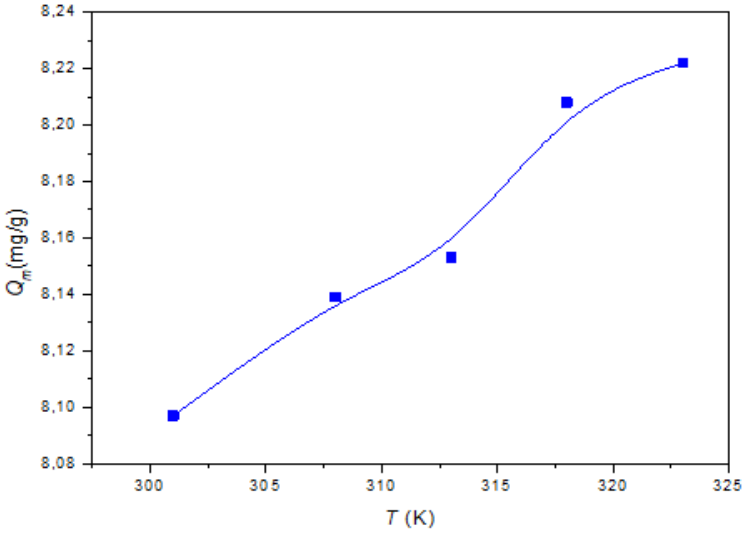

Figure 2. Maximum adsorption capacity of PAB (Q_m) vs. Temperture

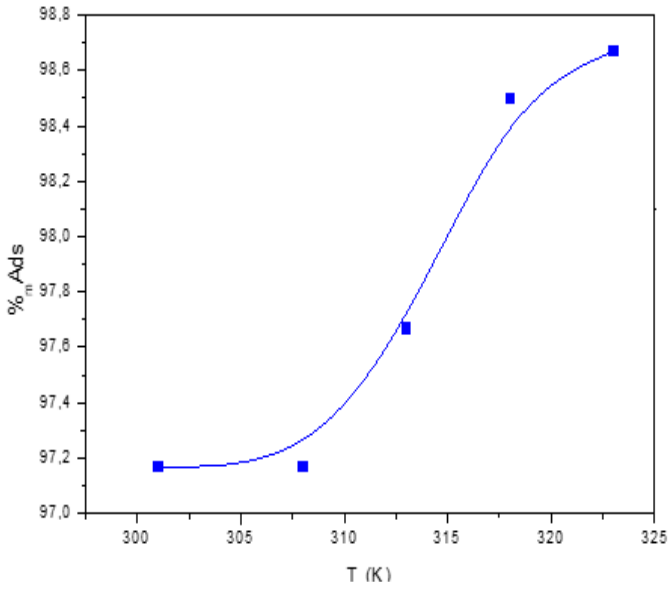

Figure 3. Maximum adsorption percentage of PAB ($\%_m Ads$) vs temperature

3.3. Contact time effect

The adsorption capacity and percentage of MB on PAB increase with contact time at different temperatures (table IV). This increase is rapid during the initial phase (first 240 minutes) and gradually decreases until it reaches a steady state (figures 4 and 5). After this steady state, indicated by a horizontal line, the adsorption capacity and percentage do not change regardless of the contact time. Thus, the maximum adsorption capacity and percentage are reached.

Table IV. Adsorption of the BM onto the PAB as a function of time at different temperatures

Time (min)	28°C		35°C		40°C		45°C		50°C	
	Q ($mg.g^{-1}$)	% Ads.	Q ($mg.g^{-1}$)	% Ads.	Q ($mg.g^{-1}$)	% Ads.	Q ($mg.g^{-1}$)	% Ads.	Q ($mg.g^{-1}$)	% Ads.
0	0.000	0,00	0,000	0,000	0.000	0,00	0.000	0,00	0.000	0,00
5	7,986	95,83	7,972	95,667	7,972	95,67	8,097	97,17	7,986	95,83
10	8,028	96,33	8,014	96,167	8,028	96,33	8,111	97,33	8,014	96,17
15	8,056	96,67	8,028	96,333	8,042	96,50	8,139	97,67	8,042	96,50
20	8,056	96,67	8,042	96,500	8,056	96,67	8,139	97,67	8,056	96,67
25	8,056	96,67	8,056	96,667	8,056	96,67	8,167	98,00	8,056	96,67
30	8,056	96,67	8,083	97,000	8,056	96,67	8,194	98,33	8,056	96,67
60	8,083	97,00	8,097	97,167	8,097	97,17	8,194	98,33	8,097	97,17
90	8,083	97,00	8,097	97,167	8,097	97,17	8,194	98,33	8,097	97,17
120	8,097	97,17	8,139	97,667	8,097	97,17	8,194	98,33	8,111	97,33
150	8,097	97,17	8,139	97,667	8,153	97,83	8,208	98,50	8,111	97,33
180	8,097	97,17	8,139	97,667	8,153	97,83	8,208	98,50	8,125	97,50
210	8,097	97,17	8,139	97,667	8,153	97,83	8,208	98,50	8,153	97,83
240	8,097	97,17	8,139	97,667	8,153	97,83	8,208	98,50	8,222	98,67
270	8,097	97,17	8,139	97,667	8,153	97,83	8,208	98,50	8,222	98,67
300	8,097	97,17	8,139	97,667	8,153	97,83	8,208	98,50	8,222	98,67
330	8,097	97,17	8,139	97,667	8,153	97,83	8,208	98,50	8,222	98,67
360	8,097	97,17	8,139	97,667	8,153	97,83	8,208	98,50	8,222	98,67
390	8,097	97,17	8,139	97,667	8,153	97,83	8,208	98,50	8,222	98,67

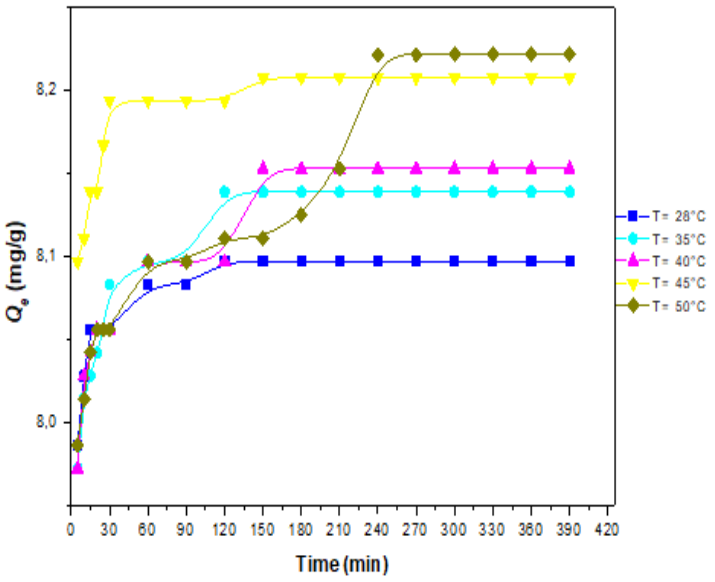

Figure 4. Equilibrium adsorption capacity (Qe) vs. time
(Co: 50 mg/L; V: 100 mL; mPAB: 600 mg).

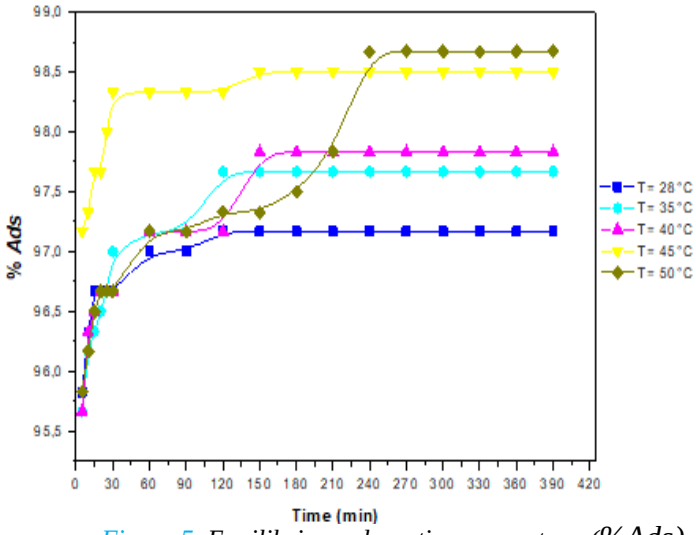

Figure 5. Equilibrium adsorption percentage (%Ads) vs. time
(Co: 50 mg/L; V: 100 mL; m_{PAB}: 600 mg).

3.4. Modeling of adsorption kinetics

The experimental data were analyzed using pseudo-first-order and pseudo-second-order kinetics. Graphs of $ln\frac{Qe}{Qe-Qt}$ and $\frac{Qt}{Qe(Qe-Qt)}$Qt as a function of time t were plotted to determine the parameters k_1, k_2, and R^2. The results obtained are presented in Table V. These results show that the overall correlation coefficients (R^2) for the pseudo-first-order and the pseudo-second-order are 0.8149 and 0.8422, respectively.

Table V. Pseudo-first-order and pseudo-second-order parameters for MB adsorption on PAB at different temperatures

T (K)	Pseudo-order 1 parameters		Pseudo-order 2 parameters	
	k_1 (min^{-1})	R^2	k_2 (min^{-1})	R^2
301	0.002	0.8031	0.802	0.8849
308	0.016	0.7599	0.227	0.8379
313	0.008	0.7340	0.108	0.8115
318	0.047	0.8848	0.699	0.7856
323	0.005	0.8928	0.038	0.8910
R^2 global		**0,8149**		**0.8422**

3.5. Adsorption isotherms

The isotherms obtained for the adsorption of MB onto PAB at different temperatures are given in figure 6. These isotherms are of S type with an initial upward concavity (at temperatures 301 K, 318 K, and 323 K)

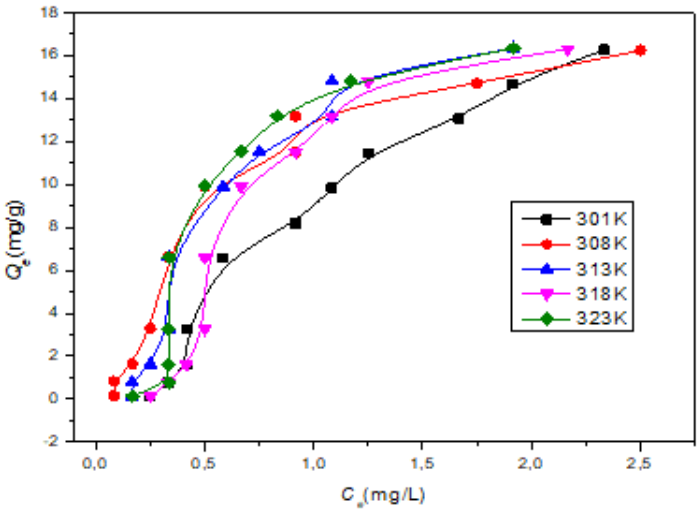

Figure 6. Adsorption isotherms of MB onto PAB at different temperatures

3.6. Modeling of Adsorption Isotherms

By linearizing the Langmuir and Freundlich equations, we were able to determine the parameters Q_m, K_L R_L, K_f, and n. The results obtained (table VI) indicate average values of 0.642 and 0.085 for 1/*n* and R_L parameters, respectively. There is a weak correlation according to the Langmuir and Freundlich models. The average correlation coefficient for the Freundlich model (R^2 = 0.7752) is slightly lower than that of the Langmuir model (R^2 = 0.7771).

Table VI. Langmuir and Freundlich parameters for the adsorption of MB onto PAB

T(K)	Q_m (mg/L)	Langmuir parameters			Freundlich parameters		
		K_L (L mg^{-1})	R_L	R^2	K_f (mg g^{-1}) (mg L^{-1})$^{-1/n}$	1/n	R^2
301	8.097	0.405	0.047	0.6909	0.298	0.384	0.6619
308	8.139	0.054	0.269	0.6864	0.309	0.477	0.7123
313	8.153	0.258	0.072	0.8553	0.161	0.683	0.8229
318	8.208	0.614	0.032	0.9724	0.087	1.044	0.8555
323	8.222	2.866	0.007	0.6807	0.287	0.623	0.8234
R^2 global			0.085	0.7771		0.642	0.7752

3.7. *Thermodynamic parameters*

The calculated thermodynamic parameters are given in table VII. The results obtained show an increase in the variation of the Gibbs free energy with increasing temperature. The variations of standard enthalpy and entropy are positive, while the variation of the standard Gibbs free energy is negative.

Table VII. Thermodynamic parameters

T (K)	$\Delta H°$ (kJ.mol^{-1})	$\Delta S°$ (kJ.mol^{-1}.K^{-1})	$\Delta G°$ (kJ.mol^{-1})	ΔG (kJ.mol^{-1})	R^2
301	+ 29.424	+ 0.169	-20.938	-21.646	0.9225
308				-22.659	
313				-23.227	
318				-24.590	
323				-25.293	

4. DISCUSSION

4.1. *Characteristics of the biosorbent PAB*

The pH_{ZPC} of PAB shows that the surface of the biosorbent is neutral at pH 4.27 (table I). Below this pH, the surface of the biosorbent is positive; above this pH, the surface of the biosorbent is negative. Other authors have also obtained acidic pH_{ZPC} values for other types of biosorbents (Bagheri et al., 2016; Mustapha et al., 2019; Adeyi et al., 2020; Litefti et al., 2024). The maximum observed adsorption capacity (Q_{mo}=31,22 mg/g) of PAB is lower than that reported by Rahimian & Zarinabadi (2020), whith 40.0 mg·g^{-1} for the pine needle biosorbent. The results given by table II show that acidic groups predominate, with a total of 1.61 meq/g. The high value obtained for the acidic functional groups would explain the acidic pH_{ZPC} (4.26) value. This indicates the acidic nature of the biosorbent.

4.2. *Temperature effect*

The increase in capacity and percentage of adsorption as a function of temperature (figures 2 and 3) is due to the diffusion of MB molecules through the boundary layer and internal pores of the adsorbent particles, following thermal agitation.

4.3. *Contact time effect*

The increase in capacity and percentage over time at different temperatures is due to the presence of a large number of free sites at the beginning, which gradually become saturated until reaching the maximum apparent adsorption capacity, represented by a horizontal floor (figures 4 and 5). At this point, the sites are saturated, and adsorption becomes constant. Other researchers have also reported the same observation (Nigist et al., 2022; Gani et al., 2023; Kifuani et al., 2024; Mateso et al., 2025; and Kifline et al., 2025).

4.4. *Adsorption kinetics*

The pseudo-second-order model provided a better fit for describing the adsorption of MB onto PAB, with a correlation coefficient (R^2 = 0.8422), compared to the pseudo-first-order model (R^2 = 0.8149) (Table V). The best fit with the pseudo-order model indicates that the adsorption is governed by the free sites of the biosorbent and the MB molecules. Similar results have been reported by Adeyi et al. (2019), Bharath et al. (2022), and Kouadio et al. (2022).

4.5. *Adsorption isotherms*

The S-shaped isotherm obtained (figure 6) indicates a vertical adsorption of the MB molecules onto the PAB biosorbent, while the L-shaped isotherm indicates a horizontal adsorption of these molecules. These results are consistent with the literature (Tahina et al., 2022; Belete et al., 2024). With a slightly higher correlation coefficient, Langmuir's model is better suited to describe the adsorption of MB on PAB (table VI). The correlation with the Langmuir model indicates that adsorption occurs preferentially in a monolayer. Belete et al., 2024, reported similar results for adsorption on other matrices. Amin et al. (2015) and Tshene et al. (2024) indicated that if the value of 1/n and R_L are less than 1, this means that adsorption is favorable. The average values of 1/*n* and R_L lower than 1 (table VI) indicate that the adsorption of MB onto PAB is favorable. The equilibrium parameter or separation parameter, R_L, indicates the affinity of the

biosorbent towards methylene blue, which can be favorable (R_L < 0), linear (R_L=1) or unfavorable (R_L> 1).

4.6. Thermodynamic parameters

The determined ΔG < 0 (Table VII) indicates the spontaneity and feasibility of adsorption. The positive Δ*H*° less than 40 kJ/mol indicates that the adsorption is endothermic and physical. The positive entropy values show that the adsorption of MB onto PAB is accompanied by an increase in disorder.

5. Conclusion

The main objective of this study was to investigate the adsorption of methylene Blue (MB) onto a biosorbent (PAB) at different temperatures. The adsorption tests were carried out in batch mode by varying different parameters. The results obtained have led to the following conclusions: The adsorption capacity and percentage of adsorption increase with contact time until reaching a constant, represented by a horizontal floor corresponding to the maximum adsorption capacity and percentage.

This increase is due to the availability of free adsorption sites on the biosorbent. The Langmuir and Freundlich models can adequately describe the adsorption of BM on PAB, and the Langmuir model was the most appropriate. The pseudo-second-order kinetic model (R^2 = 0.8422) better describes the adsorption of MB onto PAB compared to the pseudo-first-order model. The negative value of the free Gibbs energy change indicates spontaneity and feasibility of adsorption. The positive Δ*H*° less than 40 kJ/mol indicates that the adsorption is endothermic and physical.

Acknowledgments

We would like to thank the Laboratory of Physical Organic Chemistry, Water, and Environmental (LACOPE) at the Faculty of Sciences and Technology, University of Kinshasa, for providing the facilities required for this research.

Funding

This research was funded by the LACOPE Laboratory.

Conflict of interest

The authors declare that they have no competing interests.

Ethical considerations

This study was conducted in strict compliance with the ethical principles of scientific research.

Author contributions

E.O.M.: Project design, data collection, and laboratory analysis. Interpretation of results and drafting of the manuscript (first version).

A.K.M.K: Direction and coordination of the research team, review of the final version, and project approval.

B.W.T. and K.M.K.: Contribution to the mathematical and statistical processing of data and interpretation of results. Participation in the revision and correction of the manuscript.

L.L.K.: Contribution to the discussion and improvement of the manuscript.

P.B.N. and G.B.E.: Interpretation of graphs and critical review of the manuscript. Formatting of the final version of the manuscript.

Orcid of authors

Mateso O.E.: https://orcid.org/0009-0002-2349-5846

Kifuani A.K.M.: https://orcid.org/0009-0008-3677-0775

Tshene B.W.: https://orcid.org/0009-0003-1661-6766

Kifuani K.M.: https://orcid.org/0009-0005-9321-1425

Khonde, L.L. : https://orcid.org/0009-0007-8901-5100

Ngoy B.P.: https://orcid.org/0000-0001-9153-1410

Ekoko G.B.: https://orcid.org/0009-0003-1523-1741

References

Adeyi, A.A.; Jamil, S.N.A.M.; Abdullah, L.Ch.; Choong, T.S.Y.; Lau, K.L.; Abdullah, M. (2019), Simultaneous Adsorption of Cationic Dyes from Binary Solutions by Thiourea-Modified Poly(acrylonitrile-co-acrylic acid): Detailed Isotherm and Kinetic Studies. *Materials* 12(18): e2903. https://dx.doi. org/10.3390/ma12182903.

Ajala E. O., Aliyu M. O., Ajala M. A., Mamba G., Ndana A. M. et Olatunde T. S. (2024), Adsorption of lead and chromium ions from electroplating wastewater using plantain stalks modified by amorphous alumina developed from waste cans, Scientifisreports 14:6055. https://doi.org/10.1038/s41598-024-56183-2.

Alhawtali, S.; El-Harbawi, M.; El Blidi, L.; Alrashed, M.M.; Alzobidi, A.; Yin, C.-Y. (2024), Date Palm Leaflet-Derived Carbon Microspheres Activated Using Phosphoric Acid for Efficient Lead (II)

Adsorption. C, 10, 26. https://doi.org/10.3390/c10010026.

Alouani M. Alehyen S. Schouri M, Taibi M. (2018). Removel of cationic dye methylene bleue from aqueous solution by adsorption on fly ash (based geopolymer. *J. Mater. Envir. Sci*. 9(1).32-46. DOI: https://dx.doi.org/10.26872/jmes.2018.9.15.

Amal H. H. I., Nilüfer C., Neslihan I. Y., Doruk A. (2024), Adsorption of azo dye by biomass and immobilized *Yarrowia lipolytica*; equilibrium, kinetic, and thermodynamic studies, World *Journal of Microbiology and Biotechnology* (2024) 40:140 . https://doi.org/10.1007/s11274-024-039.

Amin M.T, Alazba A.A, Shafiq M., (2015), Adsorptive removal of reactive black 5 from wastewater using bentonite clay: isotherms, kinetics and thermodynamics. *Sustainability*. 7(11):15302-18.

Bagheri, A.R.; Ghaedi, M.M.; Asfaram, A.; Hajati, S.; Ghaedi, A.M.; Bazrafshan, A.; Rahimi, M.R. (2016), Modeling and optimization of simultaneous removal of ternary dyes onto copper sulfide nanoparticles loaded on activated carbon using second-derivative spectrophotometry. *Journal of the Taiwan Institute of Chemical Engineers* 65: 212-224. https://doi.org/10.1016/j.jtice.2016.05.004

Basma I. W., Israa S. Al-Bayati, Asrar A. Alobaidy, Manal A. Mohammed (2024), Adsorption Isotherms and Kinetics Studies of Lead on Polyacrylonitrile-Based Activated Carbon Nonwoven Nanofibers, *Ecological Engineering & Environmental Technology*, 25(6), 20–26 . https://doi.org/10.12912/27197050/186546.

Belete T.G., Daniel M. K. and Temesgen A. (2024), efficient removal of Methylene Blue dye from aqueous solution using a new biosorbent derived from *Ensete Ventricosum* (Enset), *Bull. Chem. Soc. Ethiop*, 38(1), 69-84.

Bharath B. G. et Senthil K. P. (2022), Adsorptive Removal of Alizarin Red S onto Sulfuric Acid Modified Avocado Seeds: *Kinetics, Equilibrium, and Thermodynamic Studies, Adsorption Science & Technology*, Vol. 2022, Article ID 3137870, 13 pages. https://doi.org/10.1155/2022/3137870.

Elie S., Guevara N., Hervé K. J. Bokossa, Crépin A., and Dominique C. K. S. (2024), Mechanism and kinetic studies of the adsorption of congo red on three adsorbent materiels, *Chemical Science International Journal.* 33 (3), 22-34. DOI: 10.9734/CSJI/2024/v33i3892.

Gani, P. Puji, L. (2023). Comparison of two biosorbent beads for methylene blue discoloration in water. *J. Ecol. Eng*., 24(8):137-145. DOI: https://doi.org/10.12911/22998993/166319.

Hajir N. S., Abdelrahman B. F., Omar A. S. (2024), Isothermal and Kinetics Investigation of Dibenzothiophene Removal from Model Fuel by Activated Carbon Developed from Mixed Date Seed and PET Wastes, *Journal of Ecological Engineering* 2024, 25(3), 38–52. https://doi.org/10.12911/22998993/177628.

Ibrahim Y. M. and Abdallah K. I. A. (2026), calculation of thermodynamic parameters, sticking probability, and apparent activation energy for adsorption of food dye e151 onto activated carbon from grape leaves, *Bull. Chem. Soc. Ethiop*., 40(6), 1281-1292.

Kifuani A.K.M., Mbemge L., Kifuani M.K., Tshene B.W., Tuluenga M.Z. (2024), Removal of a basic dye, methylene blue, from aqueous solution by adsorption onto a low-cost biosorbent made from water hyacinth (Eichhornia crassipes), *International Journal of Science Academic Rese arch*, Vol. 05, Issue 12, pp. 8728-8736.

Kifuani A.K.M., Nkiambi E.M., Kifuani K.M., Tshene B.W., and Mateso O.E. (2024), Adsorption of a basic dye, methylene blue, from aqueous solution onto a low-cost biosorbent made from peanut (Arachis hypogea) shells, *International Journal of Science Academic Rese arch*, Vol. 05, Issue 10, pp. 8454-8461.

Kifuani K.M., Kifuani A.K.M., Ilinga B.L., Ngoy P.B., Monama T.O., Ekoko G.B., and Muswema J.L. (2018a), Kinetic and thermodynamic studies adsorption of Methylene Blue (MB) in aqueous solution on a bioadsorbent from *Cucumeropsis mannii* Naudin waste seeds, *Int. J. Biol. Chem. Sci*. 12(5): 2412-2423.

Kifuani K.M., Kifuani A.K.M., Noki P.V., Ilinga B.L., Ekoko G.B., Mbala B.M., et Muswema J.L. (2018b), Adsorption d'un colorant basique, Bleu de Méthylène, en solution aqueuse, sur un bioadsorbant issu de déchets agricoles de Cucumeropsis mannii Naudin, *Int. J. Biol. Chem. Sci*. 12(1): 558-575.

Kifuani M. K, Diasonga G. G, Kifuani K.M.A, Tshene W. B., Ngoy B. P., Ekoko B.G, Ndelo-di-phanzu J. and Mukana W.M.D. (2025), Adsorption of Rhodamine B Dye from aqueous solution using an eco-friendly biosorbent from *Musa Paradisiaca* Peels: equilibrium and kinetics studies, *International Journal of Science Academic Research*, Vol. 06, Issue 10, pp. 10798-10806, October 2025

Kifuani, A.K.M. 2013. *Adsorption des composés organiques aromatiques en solution aqueuse sur charbon actif à base des déchets agroindustriels*. [Thèse de doctorat, Université de Kinshasa].

Kouadio D. L., Diarra M., Colette D.A., Dibi B., Kouamé B.D., Kone M., Karim S.T. (2022), Etude expérimentale de l'adsorption du bleu 16 et du méthyle rouge sur du charbon issu de la coque de la cabosse de cacao, *J. Soc. Ouest-Afr. Chim*, 051 : 17–30

Litefti k, Sonia M.F., Khaoula L. Mostafa S., Julia G.Á. (2024), Biosorption of methylene blue and malachite green from single and binary solutions by *pinus pinaster* BARK, *Maderas. Ciencia y tecnología* (26): 14, 1-12. DOI: 10.22320/s0718221x/2024.14.

Mateso E. O., Tshene B. W., Kifuani K. M., Kifuani A. K. M., Balaga L. B. M., Ngoy P. B., and Ekoko G. B. (2025), adsorption of a basic organic dye methylene blue in aqueous solution on a low-cost biosorbent based on *Persea americana* mill kernels, *International Journal of Science Academic Research*, 06 (03): 9653-9661.

Mekhalef B. F., Kacha, S., Leboukh, A., & Belaid, K. D. (2018). Étude comparative de l'adsorption du colorant Victoria Bleu Basique à partir de solutions aqueuses sur du carton usagé et de la sciure de bois. *Revue des sciences de l'eau / Journal of Water Science*, *31*(2), 109–126. https://doi.org/10.7202/1051695ar

Mekky AEM, El-Masry MM, Khalifa RE, Omer AM, Tamer TM, Khan ZA, Gouda M., Mohy Eldin M.S. (2020), Removal of methylene blue dye from synthetic aqueous solutions using dimethylglyoxime-modified amberlite IRA-420: kinetic, equilibrium, and thermodynamic studies. *Desalination and Water Treatment*, 181: 399-411. DOI: 10.5004/dwt.2020.25097

Merbouh C., Belhsaien K., Zouahri A., Iounes N. (2020), Evaluation De La Qualité Physico-Chimique Des Eaux Souterraines Au Voisinage De La Décharge Contrôlée Mohammedia-Benslimane : (Étude Préliminaire), European Scientific Journal, 16(6). DOI : http://dx.doi.org/10.19044/esj.2020.v16n6p455.

Mobalaji M.J, Olatunde S.D, Joshua N.E., (2021). Sequestration of hazardows dyes from aqueous solution using raw and modified agricultural waste. *Adsorption Science and Technology*, 2021: 1-21. DOI: https://doi.org/10.1155/2021/629745

Musah, B.M., Peng, L., Xu, Y. (2020), Adsorption of methylene blue using chemically enhanced Platanus orientalis leaf powder: kinetics and mechanisms. *Nat. Env. &Poll. Tech*., 19 (1): 29-40. www.neptjournal.com.

Mustapha R., (2019), *Synthèse et caractérisation d'un nouveau matériau à base de polymères*. [Thèse, Université Oran 1, Algérie].

Narayana S.K.V. and Ravi V.K. (2019), Adsorption isotherm studies on methylene blue dye removal using naturally available biosorbent, *Rasayan J. Chem*., 12(4), 2176-2182. http://dx.doi.org/10.31788/RJC.2019.1245478.

Nigist A.H., Ali S.R., and Zemene W.N. (2022), Chemical Modification of Neem (Azadirachta indica) Biomass as Bioadsorbent for Removal of Pb^{2+} Ion from Aqueous Wastewater, *Adsorption Science & Technology*, 2022-18. https://doi.org/10.1155/2022/7813513

Rahimian, R., and Zarinabadi S., (2020). A review of studies on the removal of methylene blue dye from industrial wastewater using active carbon adsorbents made from almond bark, *prog. Biochem. Res.*, 3(3):251-268. DOI: 10.33945/PCBR.2020.3.8

Raiyyaan G.D., Khalith M.S.B., Sheriff A.M., and Arunachalam K.D.A. (2021). Bioadsorption of methylene blue dye using chitosan extracted from Fenneropenaeus indicus shrimp shell waste. *J. Aquac. Mar. Biol.*, 10(4): 145-150, https://medcraveonline.com

Razia S., Syed N.T., Usman T.S., T. M. Yunus K., Shaik D.A.K., Imran M., Kiran S., M. A., Kalam H. C., Ananda M., and Akheel A.S.., (2022), Adsorption of Crystal Violet Dye from Aqueous Solution using Industrial Pepper Seed Spent: *Equilibrium, Thermodynamic, and Kinetic Studies, Adsorption Science & Technology*. Vol. 2022, Article ID 9009214, 20 pages. https://doi.org/10.1155/2022/9009214.

Tahina R. et Herizo R., (2022), Etude De Mécanisme d'Adsorption Du Colorant d'Indigo Carmin (IC) Sur Du Charbon Actif A Base De Coques De

Noix De Coco (CACC), *International Journal of Progressive Sciences and Technologies (IJPSAT)*, 39.(1) 127-135.

Tshene B.W., Kifuani K.M., Kifuani A.K.M., Ngoy P.B., and Ekoko G.B., (2024). Adsorption of a basic dye methylene blue in aqueous solution on a bioadsorbent from agricultural waste of Manihot esculenta crantz. *Int. J. Biol. Chem. Sci*. 18(3): 1180-1198. DOI: https://dx.doi.org/10.4314/ijbcs.v 18i3. 35.